sciendo
ISSN 1335-8871
MEASUREMENT SCIENCE REVIEW
Journal homepage: https://content.sciendo.com

Design and Development of Dual Band Millimeter Wave Substrate Integrated Waveguide Antenna Array

Santhakumar G[1*], Muthukumar R[2]

[1]*Department of ECE, Sri Krishna College of Technology, Coimbatore, India,* santhakumar.skct@rediffmail.com
[2]*Department of EEE, Erode Sengunthar Engineering College, Erode, India,* muthukumarr2004@gmail.com

Abstract: New communication paradigms have emerged to make better use of the available wireless spectrum due to its scarcity. Millimeter wave high-frequency spectrum could offer a viable solution to the problem of spectrum scarcity. Millimeter wave devices and antennas are becoming increasingly popular and are used in a wide variety of applications and planned Fifth Generation (5G) wireless communication networks. In this work, we develop a Substrate Integrated Waveguide (SIW) based antenna array and millimeter-wave feeding network with the aim of achieving optimal performance. A microstrip array antenna is developed for use at millimeter wave frequencies of 28 GHz and 38 GHz. Next, an SIW array antenna will be created. For high-frequency uses, SIW technology excels due to its low loss, easy integration and high quality factor. The two unequal longitudinal slots in a slotted SIW antenna cause the structure to resonate at 28 GHz and 38 GHz. The SIW structure is fabricated by making two parallel rows of metallic vias, carefully determined through sizes to ensure minimal internal losses. A microstrip line that transitions into a SIW feeds into the proposed layout. In this paper, the authors investigate the design and construction of an integrated waveguide antenna array for use at dual millimeter-wave frequencies.

Keywords: Dual band, frequency, antenna, micro strip array.

1. INTRODUCTION

The term "wireless communication" refers to a method of transmitting and receiving data without the need of a physical link such as cable, wire, fiber optics or other electrical conductors. It is the backbone of any interconnected terrestrial and space-based national communications infrastructure [1]-[3]. The 'antenna' is a radiating device that is crucial for establishing radio communication between the sending and receiving ends. Synchronized progress in antenna technology is required for the development and implementation of developing telecommunication systems due to advances in electronic device technology, switching technology, and the availability of a new radio spectrum for telecommunication services [4]-[6].

Today's telecommunications infrastructure is stretched to its limits by a wide range of data, telephone, video and other types of traffic. As a result, enormous channel bandwidth is needed to provide integrated high-speed services for new technologies such as the Internet of Things, big data analytics, block chain, etc. [7]-[10].

Substrate Integrated Waveguide (SIW) operates at higher frequencies, has a higher quality factor, can handle more power and can be more easily integrated into other circuits than rectangular waveguide [11]-[14].

2. MATERIAL AND METHODS

Fig. 1 shows the steps used to create the elliptical patch antenna. To create an antenna that resonates at a specific frequency, one must first determine the precise measurements required to build the antenna. Selecting a substrate and determining the parameters of the design is the first step. The next step is to plan the layout of an elliptical patch and the feed lines. Feedback from the simulation results and the prototype tests were used to iteratively refine the design so that each version of the antenna improved on the previous one. A multilayer patch antenna array with four elements is then built. Reliability and durability are ensured by selecting materials and design specifications that meet industry standards for environmental resistance. A transition from coaxial to microstrip line is used to power the proposed antenna array. Computer Simulation Technology (CST) software is used to simulate of the proposed design.

A. Patch ellipse calculation

The semi major axis a, the semi minor axis b and the effective semi major axis a_{eff} are the coordinates that define the elliptical patch according to (2). For a patch with a radius, this is the only possible range according to (3). The primary mode of the elliptical patch is Transverse Magnetic Waves (TM_{11}).

The resonant frequency f_r of the dominant mode TM_{11} is given by (1):

DOI: 10.2478/msr-2024-0014

*Corresponding author: santhakumar.skct@rediffmail.com(Santhakumar G)

$$f_{r11} = \frac{x'_{mn} v_o}{2\pi a \sqrt{\varepsilon_r}} \quad (1)$$

where v_o is the speed of light in empty space, x'_{mn} is the derivative of the Bessel function and is equal to 1.8412, ε_r is the relative permittivity and a is the semi major axis.

To determine the effective semi major axis a_{eff} :

$$a_{eff} = a\left[1 + \frac{2h}{a\pi\varepsilon_r}\left\{ln\left(\frac{\pi a}{2h}\right) + 1.7726\right\}\right]^{1/2} \quad (2)$$

where h is the height of the substrate.

From the above equation, the value for a_{eff} is 2.1 mm.

The size of the patch is determined by:

$$a = \frac{F}{\left[1+\frac{2h}{\pi\varepsilon_r F}\left\{ln\left(\frac{\pi F}{2h}\right)+1.7726\right\}\right]^{1/2}} \quad (3)$$

where

$$F = \frac{8.791 \times 10^9}{f_r \sqrt{\varepsilon_r}}$$

Frequency, F = 28.5 GHz, with a = 1.8 using (3). f_r is the resonant frequency.

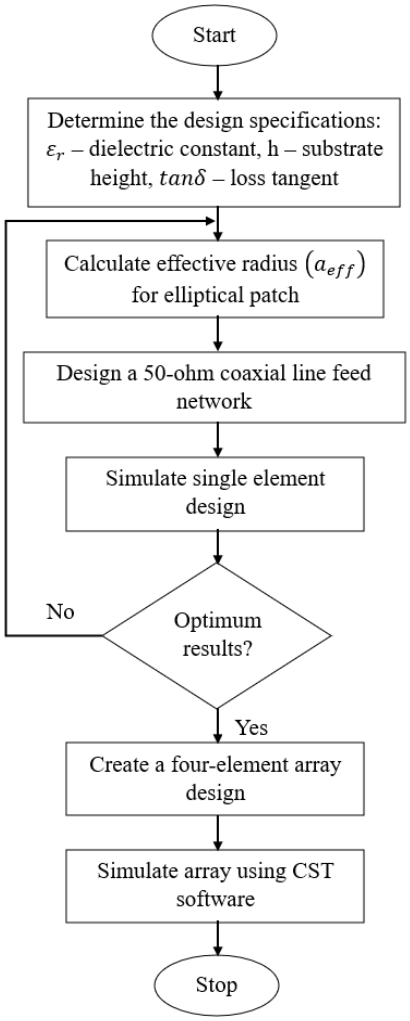

Fig. 1. Microstrip patch array antenna design flowchart.

B. Material for the antenna design

Millimeter wave frequencies from 30 GHz to 300 GHz make the construction of circuits very challenging. The substrate used is Rogers Reverse Treated (RT)/duroid 5880, with a loss tangent $tan\ \delta$ of 0.003, a permittivity ε_r of 2.2 and a height of 0.254 mm. The proposed single SIW element antenna measures 30 × 7.50 × 0.254 mm (length × width × height). Millimeter waves have a very narrow frequency range, from 30 GHz to 300 GHz, and a very short wavelength, from 1 to 1000 mm. Due to the signal's susceptibility to attenuation and atmospheric losses, mm-wave communications are limited to short-range usage. To reduce losses at high frequencies, a substrate material with low dissipation is preferred. The quality of the conductor surface can play a significant role in millimeter-wave losses. For example, a rough copper surface can lead to considerable conductor losses compared to a clean surface. Rogers Corporation's RT/duroid 5880, which is made from glass microfiber-reinforced polytetrafluoroethylene (PTFE) composites, emerged as a winner in a comparison of many competing materials. The low dielectric constant and low dielectric losses make Rogers RT/duroid ideal for use in high-frequency applications. At 10 GHz, the dielectric constant and dissipation factor of this material are 2.2 and 0.0009, respectively. It is isotropic and absorbs very little moisture. RT/duroid is simple to form by trimming, cutting and milling. They can withstand the heat and cold of the liquids and reactants used to etch Printed Circuit Board (PCB) and holes.

C. Design of a dual band antenna

In order to maintain a small form factor in high-frequency devices, the need for dual-band or multi-band antennas is increasing. First, we will talk about a patch antenna and its use in millimeter wave communication. Then we will introduce the antenna equipped with SIW technology to achieve excellent antenna performance at high frequencies.

D. Microstrip patch antenna

In this study, an elliptical patch microstrip antenna is designed for use at 28 GHz and 38 GHz. Fig. 2 shows how the proposed design of a single-element and array antenna could look like. The proposed antenna utilizes a Rogers RT/duroid substrate material that has a dielectric constant of 2.2 and a loss tangent of 0.003. The proposed configuration is an elliptical slot coaxially fed along its major and minor axes, a and b. The dimensions and configurations have been optimized based on simulation results to achieve the desired dual-band operation with minimum interference and maximum efficiency, as shown in Table 1.

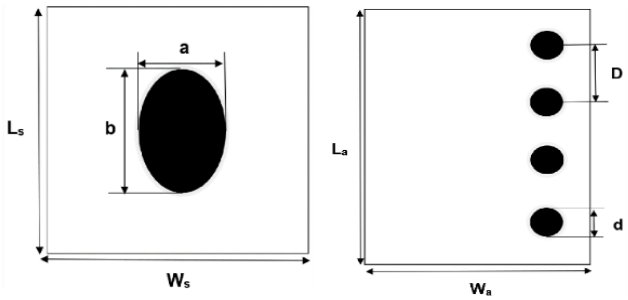

(a) (b)

Fig. 2. Single elliptical patch antenna (a) and a 4-element array (b).

Table 1. The suggested microstrip patch antenna's dimensions and tuning parameters.

Parameters	*Ls*	*Ws*	*h*	*b*	*a*	*R*	*Lf*	*Wf*
Dimension [mm]	10	10	0.25	3.96	2.68	2.39	9	0.75
Description	Substrate length	Substrate width	Substrate height	Major axis diameter (y-direction)	Minor axis diameter (x-direction)	Patch radius	Center feed length	Center feed width

Table 2. Specifications for the single-element, wideband antenna.

Parameters	*L*	*W*	*L1*	*W1*	*L2*	*W2*	*Lt*	*Wt*	*Lf*	*Wf*
Dimension [mm]	30	7.5	6.54	0.7	4.22	0.17	6.1	3	3.5	0.75
Description	Substrate length	Substrate width	Length of first Slot	Width of first Slot	Length of second Slot	Width of second Slot	Transition section length	Transition section width	Feed line length	Feed line width

E. SIW antenna

First, two rows of metallic vias are produced for the SIW structure design. When designing SIW, the size and location of the through holes are crucial. The diameter of the vias (*d*), the distance between neighboring vias (*p*) and the distance between two rows of vias (SIW) are the most important determinants for the SIW design. The two slots running at 28 and 38 GHz are placed longitudinally in the conduction plane. To power the proposed antenna, a microstrip to SIW adapter is used. There is a break near the transition section to allow the impedances to be balanced. High-frequency operation requires a substrate with a low dielectric constant. A Rogers RT/duroid 5880 substrate is used here because of its low loss tangent (0.003) and a high dielectric constant (2.2). The measurements for the proposed SIW layout are shown in Table 2.

F. Design steps

The following procedures are used in the design of the proposed SIW antenna in the CST software:

- *Material for the substrate is selected*
  The dimensions of the Rogers RT/duroid 5880 substrate material are 30 × 7.50 × 0.254 mm (length × width × height) after the CST microwave studio is opened.
- *Deciding between the primary and secondary layers*
  The conductive layers on the top and bottom were made with the same dimensions as the selected substrate.
- *Feed line*
  Impedance matching is achieved by microstrip tapering of the 50-feed line. *Lt* = 6.1 mm and *Wt* = 3.0 mm are the dimensions of the taper.
- *Conductive plane with longitudinal slots*
  Two unequal longitudinal grooves were carved into the conducting plane to allow the antenna to resonate at 28 GHz and 38 GHz. The dimensions for slot 1 are 6.54 mm in length (*L1*) and 0.70 mm in width (*W1*), while the dimensions for slot 2 are 4.22 mm in length (*L2*) and 0.17 mm in width (*W2*).
- *The design of an SIW*
  The integrated waveguide structure is produced after the slots are etched on a substrate. The SIW structure consists of two parallel rows of cylinder-shaped vias with a diameter (*d*) of 0.5 mm and a pitch (*p*) of 1.0. The novelty lies in the integration of unequal longitudinal slots to achieve efficient dual-band operation at 28 GHz and 38 GHz, optimized for the emerging 5G networks.

3. RESULTS

A. Designing a microstrip patch antenna

In this section, all simulation results for an elliptical patch antenna with a single-element and array-system are described in detail.

Return loss (S_{11})

Fig. 3 shows the simulated return loss graph together with the bandwidth range for a single element. The plot shows the return loss as a function of frequency between 28 GHz and 38 GHz. The -17.61 dB return loss at 28 GHz and the -14.62 dB return loss at 38 GHz were both achieved. The frequency ranges covered by the proposed dual band antenna design are (27.83-28.51) GHz and (37.56-38.84) GHz with a bandwidth of -10 dB. The return loss in the 28 GHz and 38 GHz bands for the array of four components is shown in Fig. 4. The simulated -10 dB bandwidth for the array design spans the frequency ranges of (37.32-38.80) GHz and (27.79-28.70) GHz. For 38 GHz and 28 GHz, the measured return loss is -15.59 dB and -22.32 dB, respectively.

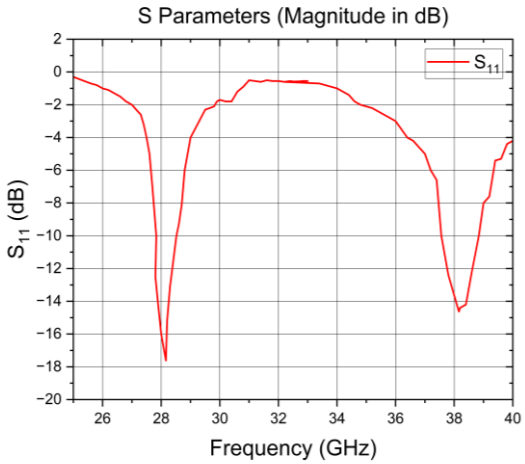

Fig. 3. Return loss for a single-element patch antenna.

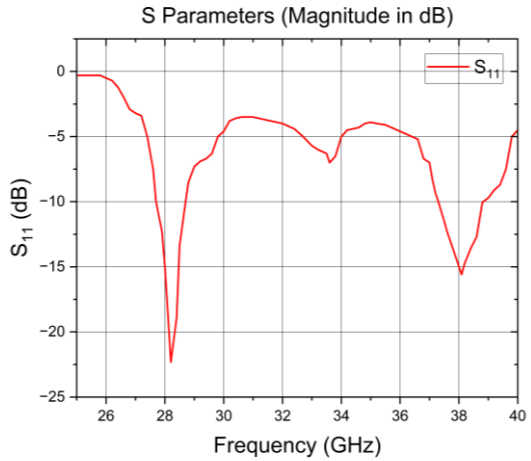

Fig. 4. Return loss for a 38 GHz and 28 GHz patch antenna array.

B. *Waveguide antennas integrated into the substrate*

In this part, the modeling results for a single element and an array structure of a slotted substrate integrated waveguide antenna are presented.

This effect on antenna performance was designed due to the use of through holes in SIWs. In addition, two uneven longitudinal slits were cut in the conducting plane to improve the antenna's characteristics. The simulation was performed using CST microwave studio.

C. *Single element slotted SIW antenna*

Return loss (S_{11})

Fig. 5 shows the return loss versus frequency plot for a single element SIW antenna with an impedance bandwidth of -10 dB between 28 GHz and 38 GHz. It has a bandwidth of 3.2% over the frequency range of (27.6-28.5) GHz at 28 GHz and 1.3% over the range of (37.8-38.3) GHz at 38 GHz. At 28 GHz, we measured a return loss of 18.41 dB and at 38 GHz a return loss of -20.159 dB. The graph clearly shows that the return loss is reduced by using a slot and vias instead of a patch antenna.

D. *Antenna array with 4 SIW components (1×4)*

The four elements of the antenna are designed to work together for maximum gain. This structure is connected to the corporate feed network to improve the antenna array's efficiency.

Return loss (S_{11})

Fig. 6 shows the return loss graph of the array antenna. At both 28 GHz and 38 GHz, the array has a return loss of less than -10 dB. The bandwidth between (27.6-28.1) GHz is 0.5 GHz and the resulting return loss is -14.92 dB at 28 GHz.

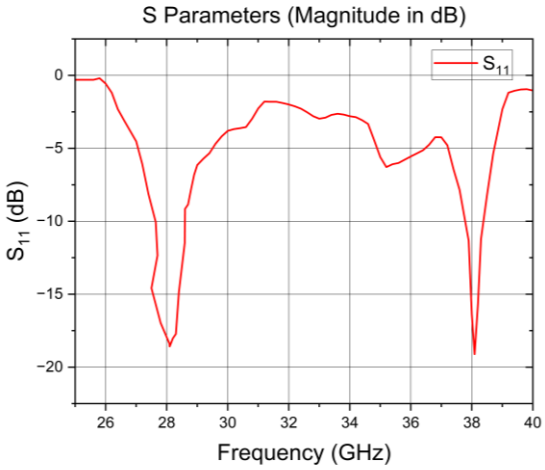

Fig. 5. Return loss for a single slotted in-plane element.

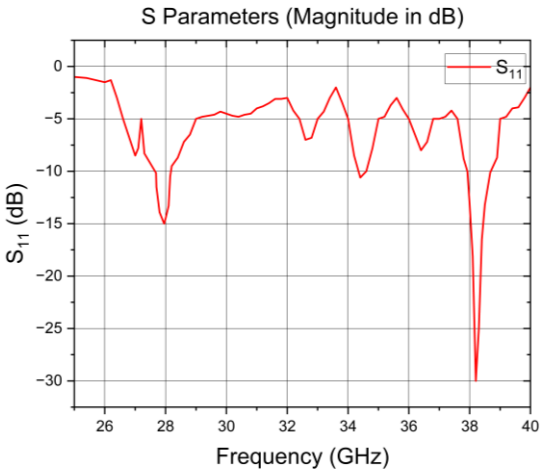

Fig. 6. Antenna array for an SIW return loss.

E. *Comparative analysis*

The simulation results for the proposed microstrip patch antenna and the SIW antenna are compared here for the first time. Table 3 shows the results of an investigation and comparison between the design of the proposed SIW antennas and the aforementioned research articles and reference documents.

Table 3. Microstrip patch antenna versus SIW antenna comparison.

Parameter	Frequency (f_r) = 28 GHz				Frequency (f_r) = 38 GHz			
	Single element		Antenna array		Single element		Antenna array	
	Patch	SIW	Patch	SIW	Patch	SIW	Patch	SIW
Return loss [dB]	-17.61	-18.84	-22.32	-13.70	-14.62	-20.16	-15.59	-30.13
Bandwidth [%]	2.43	3.20	3.22	1.80	3.30	1.30	3.33	2.06
Efficiency [%]	76.96	94.90	82.41	90.48	89.86	89.14	81.94	83.78

4. DISCUSSION

A four-element antenna array is created by extending the single-element antenna design. The T-junction power divider is used to distribute power from a corporate feed network to the array. Each element of the array receives the same amount of electricity thanks to this feed network. Both the efficiency and the gain for these array systems are quite respectable. The results show that the return loss is quite low across the studied frequency ranges, with mean values of -13.7 dB and -18.12 dB at 28 GHz and 38 GHz, respectively. The proposed four-element antenna array has a fractional bandwidth of 1.8% over the frequency range of (27.6-28.1) GHz and 2.06% over the frequency range of (37.9-38.67) GHz, both of which are quite high and sufficient for wireless communication.

5. CONCLUSION

For the Ka-band frequency range, a SIW-based slotted antenna array was developed. The antenna's resonant frequencies of 28 GHz and 38 GHz are generated by these slots. A gap is then positioned close to the transition region of the microstrip to the SIW to ensure good impedance matching. The simulation results show that the antenna has a return loss of less than -10 dB for both frequency bands. Future work will investigate bandwidth and efficiency improvements, integration with advanced beamforming networks for improved directional control, and adaptation of the design to support additional frequency bands, potentially extending its applicability to 6G and other high-frequency applications.

DATA AVAILABILITY STATEMENT

Available Based on Request. The datasets generated and/or analyzed during the current study are not publicly available due to the extension of the submitted research work. They are available from the corresponding author upon reasonable request.

REFERENCES

[1] Parveez Shariff, B. G., Mane, P. R., Kumar, P., Ali, T., Nabi Alsath, M. G. (2023). Planar MIMO antenna for mmWave applications: Evolution, present status & future scope. *Heliyon*, 9 (2), e13362. https://doi.org/10.1016/j.heliyon.2023.e13362

[2] Sehrai, D. A., Khan, J., Abdullah, M., Asif, M., Alibakhshikenari, M., Virdee, B., Shah, W. A., Khan, S., Ibrar, M., Jan, S., Ullah, A., Falcone F. (2023). Design of high gain base station antenna array for mm-wave cellular communication systems. *Scientific Reports*, 13 (1), 4907. https://doi.org/10.1038%2Fs41598-023-31728-z

[3] Ahmad, A., Choi, D. (2022). Compact eight-element MIMO antenna with reduced mutual coupling and beam-scanning performance. *Sensors*, 22 (22), 8933. https://doi.org/10.3390%2Fs22228933

[4] Lu, S., Qu, S.-W. (2023). Low-profile dual-band reflector antenna for high-frequency applications. *Sensors*, 23 (13), 5781. https://doi.org/10.3390/s23135781

[5] Bhatia, S. S., Sivia, J. S., Sarao, A. K. (2022). Lantern logo shaped novel monopole antenna with semi-circular notch loaded partial ground plane for ultra-wideband wireless applications. *Wireless Personal Communication*, 126, 3211-3231. https://doi.org/10.1007/s11277-022-09860-2

[6] Sidhu, A. K., Sivia, J. S. (2024). Design of a novel 5G MIMO antenna with its DGP optimisation using PSOGSA. *International Journal of Electronics*, 111 (1), 105-126. https://doi.org/10.1080/00207217.2022.2148288

[7] Zhu, J., Yang, Y., Mcgloin, D., Liao, S., Xue, Q. (2021). 3-D printed all-dielectric dual-band broadband reflectarray with a large frequency ratio. *IEEE Transactions on Antennas and Propagation*, 69 (10), 7035-7040. https://doi.org/10.1109/TAP.2021.3076528

[8] Jin, L., Tang, H., Shi, J., Lin, L., Xu, K. (2022). A dual-band, dual-polarized filtering antenna based on cross-shaped dielectric strip resonator. *Micromachines*, 13 (12), 2069. https://doi.org/10.3390/mi13122069

[9] Armagan, O., Kahriman, M. (2022). The effect of the co-planar structure on HPBW and the directional gain at the square patch antenna around ISM 2450 MHz. *Technical Gazette*, 29 (4), 1120-1125. https://doi.org/10.17559/TV-20190423010908

[10] Cao, Y. F., Zhang, X. Y., Xue, Q. (2022). Compact shared-aperture dual-band dual-polarized array using filtering slot antenna and dual-function metasurface. *IEEE Transactions on Antennas and Propagation*, 70 (2), 1120-1131. https://doi.org/10.1109/TAP.2021.3111179

[11] Ganesan, R., Panchavarnam, M. V., Thangaiyan, J. (2023). Split ring resonator inspired dual-band monopole antenna for ISM, WLAN, WIFI, and WiMAX application. *Technical Gazette*, 30 (5), 1533-1538. https://doi.org/10.17559/TV-20230210000344

[12] Xu, K., Jin, L., Tang, H., Yang, W.-W., Shi, J. (2022). A high-efficiency dual-band self-filtering antenna based on three dense dielectric strip resonators. *IEEE Antennas and Wireless Propagation Letters*, 21 (8), 1532-1536. https://doi.org/10.1109/LAWP.2022.3173378

[13] El houda Nasri, N., EL Ghzaoui, M., Fattah, M. (2024). A quad port MIMO antenna with improved bandwidth and high gain for 38 GHz 5G applications. *Franklin Open*, 6, 100078. https://doi.org/10.1016/j.fraope.2024.100078

[14] Parveez Shariff, B. G., Ali, T., Mane, P. R., Kumar, P., Pathan, S. (2024). Compact wideband two-element millimeter wave MIMO antenna with CMT based modified T-shaped decoupling structure for mobile applications with estimated link budget in urban scenario. *AEU - International Journal of Electronics and Communications*, 177, 155209. https://doi.org/10.1016/j.aeue.2024.155209

Received October 2, 2023
Accepted April 29, 2024